Journal of Thermal Science Vol.29, No.3 (2020) 708–717

https://doi.org/10.1007/s11630-020-1212-7 **Article ID: 1003-2169(2020)03-0708-10**

Effect of Nanoparticle Type and Surfactant on Heat Transfer Enhancement in Spray Cooling

WANG Bingxing, LIU Zhixue*, ZHANG Bo, XIA Yue, WANG Zhaodong, WANG Guodong

The state key laboratory of rolling and automation (RAL), Northeastern University, Shenyang 110819, China

Abstract: In this study, the heat transfer characteristics of nanofluids used in spray cooling systems were examined. Three nanofluids, i.e., Cu, CuO, and Al_2O_3, respectively, with volume fractions ranging from 0.1% to 0.5%, as well as different volume fractions of a surfactant Tween 20, were used. In addition, their contact angles were measured to examine the heat-transfer characteristics. Under the same experimental conditions, with the increase in the volume fraction of the Cu nanoparticles from 0.1% to 0.5%, the maximum heat flux q_{max} increased from 3.36 MW/m^2 to 3.48 MW/m^2 from the impinging central point to r=30 mm (r is the distance from the impingement point), and the corresponding temperature of q_{max} increased from 400°C to 420°C. Results revealed that with increasing Tween 20 concentrations, the contact angle decreased because of the decrease in the surface tension of nanofluids and improvement of the wetting ability, and the corresponding q_{max} increased from 3.48 MW/m^2 to 3.94 MW/m^2 at the impact central point.

Keywords: spray cooling, nanofluids, surfactant, wettability, heat flux

1. Introduction

Spray cooling plays a vital role in nuclear reactors, coal gasification, electronic chips and metal heat treatment. In the steel industries, the steel strips strength properties and the microstructure are greatly influenced by the cooling ability in the run-out table [1]. The steel plate with high temperature above 900°C, microstructure and the heat transfer characteristic during the cooling process is interrelated with the boiling phenomenon [2]. When the vapour droplets impact on the surface of the steel plate, film boiling heat transfer, transition boiling heat transfer, nucleate boiling heat transfer and single-phase forced convection heat transfer will occur.

Spray droplet flux distribution [3] and diameter [4], mass flux, inclination angle [5], surface temperature and coolant subcooling [6], affect the spray cooling performance, i.e., heat flux, heat transfer coefficient, cooling efficiencies, rewetting temperature, wetting delay [7], and thin liquid film flow [3]. And the surfactant [8] and nanofluid additives [9] both enhance the heat transfer of air-atomized spray cooling on hot steel plate.

Studies on the effects of nanoparticles and surfactants on spray cooling performance are rare. Kolsi et al. [10] and Rashed et al. [11] both have found the total entropy generation increases with increasing of Rayleigh number and reducing of solid volume fraction of nanofluid. Wongcharee et al. [4] have experimentally examined nanofluids with different TiO_2 concentrations of 0.5%–2.5% under swirling impinging jets and reported that 0.5%–2% nanofluids exhibit a higher Nusselt number compared to 2.5% nanofluids. Fan et al. [12] have reported the enhancement of the critical heat flux using various concentrations of graphene-based aqueous

Received: Sep 25, 2018 Corresponding author: LIU Zhixue E-mail: a947437732@163.com

Nomenclature

a	thermal diffusivity/$m^2 \cdot s^{-1}$	T_a	actual temperature/K
C	specific heat capacity/$J \cdot kg^{-1} \cdot K^{-1}$	T_c	calculation temperature/K
q	heat flux/$MW \cdot m^{-2}$	T_{max}	temperature at maximum heat flux/K
q_{max}	maximum heat flux/$MW \cdot m^{-2}$	t	the time/s
r	the distance from the impingement point	t_{max}	the time at maximum heat flux/s
T	temperature/K	x	thickness/m

nanofluids, corresponding to the increase in the nucleation site density and liquid agitation intensity. Karimzadehkhouei et al. [13] have reported that nanofluids containing TiO_2 nanoparticles exhibit a higher heat flux compared to CuO nanofluids, while the heat transfer augments decrease with mass fraction. Sundar et al. [14] have reported that the heat transfer enhancement of hybrid nanofluids is considerably more striking than single-nanoparticle-based nanofluids or conventional fluids. Lee et al. [15] has numerically investigated the effect of spray height, nanofluid type, and nanofluid concentration and reported that the increase in the spray height decreases the heat transfer at low nanofluid concentrations at a nanofluid concentration ranging from 0.5% to 2.5%. Jay et al. [16] have examined the effects of surfactant on nanofluids and measured the thermo-physical properties of four coolants and reported that surfactant increase the cooling ability of nanofluids. Mohapatra et al. [17,18] studied the enhancement of heat transfer during the surfactant water jet impingement cooling. Their research focused on the increase of cooling rate of stainless steel plate at different of surfactant concentrations. It is found that an increase in surfactant concentration increases the cooling rate. Clay et al. [19] found that a decrease in surface tension causes a decrease in contact angle, causing an increasing number of bubble nucleation sites enhancing the wetting capacity of coolant on the surface [20]. Therefore, from the above literature, it is found that surface tension, contact angle and nanoparticle type play a promising role in the enhancement of heat transfer.

In the current study, concentration and surfactant on surface tension and contact angle has been primarily examined as a fundamental research on heat transfer enhancement. Secondly, air-atomized spray cooling of a hot stainless steel plate has been done with different concentration and different nanoparticle to calculate the heat flux. The surfactant used is Tween 20, because the non-ionic surfactant induces less foaming, and its effect on the surface tension and contact angle is pronounced. The cooling study has been carried out from an initial temperature of 700°C, which is beyond the Leidenfrost point.

2. Experimental Setup and Procedure

2.1. Experimental device and procedure

Fig. 1 shows the experimental device, including a gas supply system, h eating system, data acquisition system, water pump, steel plate, spray nozzles, and a flow meter. The water flow ranged from 1.5 L/min to 30 L/min, and the pressure range of the air compressor was 0–0.8 MPa, which was measured using a barometer. The distance from the spray to the target was adjusted from −400 mm to 400 mm.

The experimental steel plate is heated to 720°C to prevent the temperature reduction of steel plate in the process of movement; then the steel plate is placed on the experimental platform, and cover the steel plate with a baffle, opening the flow valve, adjust it to the required flow; what' more, open the air pump, adjust the pressure valve to the required pressure; Last, remove the baffle when the vapor mist stabilizes quickly.

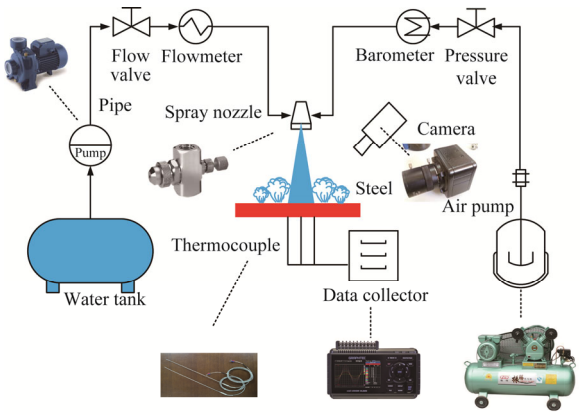

Fig. 1 Experimental facility platform

The AISI 304 steel plate size was 150 mm × 80 mm × 20 mm, and 4 holes at 2.5 mm below the surface of the steel plate, which the diameter is 3mm; the hole depth was 30 mm; and the distance between two adjacent holes was 10 mm. In addition, inserted the type K Chromel–Alumel thermocouples into the holes, and seal the gap with high-temperature glue YK-8908 (Fig. 2). P1-P4 is the thermocouple position. The Graphtec GL220 was used to collect the data at a sampling frequency of 100 ms.

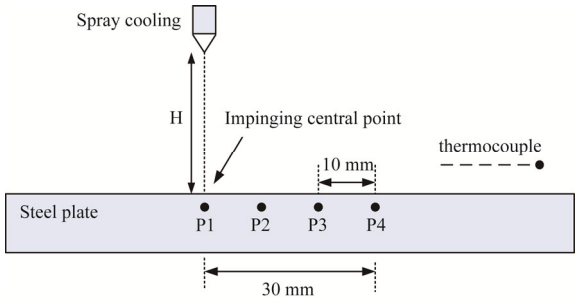

Fig. 2 Thermocouple arrangement of Jet impingement

To analyze the wettability of nanofluids, different nanofluids prepared in the laboratory were analyzed by an OCA 15PRO contact angle meter.

2.2. Preparation of nanofluids

A previously reported method [21] was used to prepare nanofluids required for the experiment, and the details were as follows. An electronic balance was used to weigh Cu, CuO, and Al_2O_3 nanoparticles with a particle granularity of 20–50 μm, followed by mixing deionized water. Next, Tween 20 as the surfactant was added, and carried out ultrasonic oscillation, with final ultrasonic oscillation for ~1 h. By using the above method, Cu, CuO, and Al_2O_3 nanofluids with volume fractions of 0.1% and 0.5% were prepared; correspondingly, nanofluids were prepared by the addition of 100 mg/L, 300 mg/L, and 600 mg/L of Tween 20 into the Cu nanofluids with a volume fraction of 0.5%. Table 1 summarizes the specific experimental parameters.

Experiments were carried out with different nanofluids and different volume fractions to examine the effect of the heat exchange process. Seven groups of experiments with a flow rate of 0.3 L/min were designed at an air pressure of 0.2 MPa and an initial temperature (temperature at the beginning of cooling) of 700°C. Table 2 summarizes experimental parameters.

Table 1 Experimental parameters of different nanofluids

Solute	Solvent	Volume fraction /%	Surfactant concentration /mg·L^{-1}
Cu	deionized water	0.1	-
Cu	deionized water	0.5	-
CuO	deionized water	0.1	-
CuO	deionized water	0.5	-
Al_2O_3	deionized water	0.1	-
Al_2O_3	deionized water	0.5	-
Cu	deionized water	0.5	100
Cu	deionized water	0.5	300
Cu	deionized water	0.5	600
-	deionized water	-	-
-	deionized water	-	600

2.3. Calculation method

Table 3 summarizes the parameters of AISI 304 steel plate. The energy conservation equation and heat conduction equation of the plate cooling process were expressed as follows:

$$\rho c \frac{\Delta T}{\Delta t} = \Delta\left(k \Delta T\right) \tag{1}$$

The heat conduction issue was abstracted into one dimension, which was simplified as follows:

$$\frac{\partial T}{\partial t} = a \frac{\partial^2 T}{\partial x^2} \qquad (0 < x < h, t > 0) \tag{2}$$

Initial condition: $T(x,0)=f(x)$ $(0 \le x \le h)$

Table 2 Experimental parameters

Case	Solute	Solvent	Surfactant concentration/mg·L^{-1}	Flow rate /L·min^{-1}	Air pressure /MPa	Initial temperature/°C
E1	0.1%Cu	deionized water	-	0.3	0.2	700
E2	0.5%Cu	deionized water	-	0.3	0.2	700
E3	0.1%CuO	deionized water	-	0.3	0.2	700
E4	0.5%CuO	deionized water	-	0.3	0.2	700
E5	0.1%Al_2O_3	deionized water	-	0.3	0.2	700
E6	0.5%Al_2O_3	deionized water	-	0.3	0.2	700
E7	-	deionized water	-	0.3	0.2	700
E8	-	deionized water	600	0.3	0.2	700
E9	0.5%Cu	deionized water	100	0.3	0.2	700
E10	0.5%Cu	deionized water	300	0.3	0.2	700
E11	0.5%Cu	deionized water	600	0.3	0.2	700

Boundary condition:

$$-\lambda(T)\frac{\partial T(x,t)}{\partial x}=q_{\mathrm{i}}+q_{\mathrm{r}}$$

where, a is the thermal diffusivity, m^2/s; T is the temperature; k is thermal conductivity; ρ is density; c is the specific heat; τ is the time, s; x is the thickness, m; h is the steel plate thickness, m; q_{i} is the heat flux of the spray, W/m^2; and q_{r} is the heat flux of thermal radiation, W/m^2.

The finite difference method was employed to solve the heat conduction problem. The absolute value of the difference between measured and calculated values was δ=0.01°C.

Fig. 3 shows the flow chart showing the reverse heat transfer calculation.

where, T_{a} is the actual temperature; T_{c} is the calculation temperature.

2.4. Measurement uncertainty

Two typical uncertainties in any measurement, i.e., random and systematic, exist. Each experiment was repeated thrice to reduce the experimental error. The result data is the average data of each experiment. The measured temperature and coolant flow rate were the main sources of uncertainties in the study. The error of type K thermocouples was about ±2°C. The relative error of the temperature acquisition system was ±0.5%. In addition, the cumulative error in the inverse calculation of the heat flux was within ±2%.

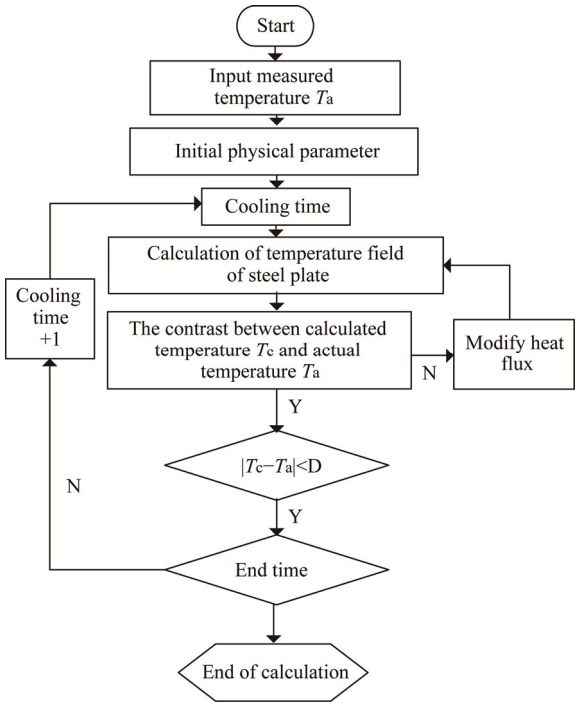

Fig. 3 Flow chart showing the reverse heat transfer calculation

Table 3 Parameters of AISI 304

Temperature T/ °C	Thermal diffusivity a/ $cm^2 \cdot s^{-1}$	Specific heat capacity C/ $J \cdot kg^{-1} \cdot K^{-1}$	Thermal conductivity λ/ $W \cdot m^{-1} \cdot K^{-1}$
20	0.0319	476	11.93
100	0.0333	483	12.64
200	0.0352	491	13.58
300	0.037	500	14.54
400	0.0388	508	15.49
500	0.0406	518	16.53
600	0.0424	529	17.63
700	0.042	543	18.86
800	0.0479	588	22.14
900	0.0479	588	22.14

3. Results and Discussion

3.1. Analysis of wettability of nanofluids

Fig. 4 shows the 100-fold of contact angles of nanoparticles with different concentrations and surfactant, and pictures of 0 s, 9 s and 27 s were selected, because the moment when the droplet completely drops to the base surface at 0 s. The contact angles of different nanofluids and their volume fractions first decreased and then remained stable, indicating that the surface tension of the liquid droplets increases for wetting (Fig. 4). By the comparison of Fig. 4(a) and (b), (c), and (d), (e), and (f), with the increase of the nanoparticle volume fraction in nanofluids from 0.1% to 0.5%, the solid/liquid contact angles of Cu, CuO, and Al_2O_3 nanofluids increased from 93.2°, 104.7°, and 89.8° to 105.4°, 106.9°, and 100.3°, respectively, at 0 s, corresponding to the relative viscosity of nanofluids with the increase in the nanoparticle volume fraction [8]. High viscosity will increase the friction between colloidal particles in solution, and surface tension will retard the propagation of wetting.

With the addition of 600 mg/L of Tween 20 into deionized water, the contact wetting angle gradually decreased from 81° to 70.7° with the increase in the time to 27 s, and its wettability was better than that of deionized water. Owing to the decrease in the polarity of deionized water by the addition of Tween 20, the rewetting velocity is increasing [22]. Furthermore, the surface tension decreased as the surfactant concentration increases [23].

With the decrease in the surfactant concentration from 600 mg/L to 100 mg/L, the contact angle increased from 83.7° to 92.3° at 0 s for the Cu nanofluids with a volume fraction of 0.5% (Fig. 4(i), (j), (k)). On the other hand, by using 600 mg/L surfactant Cu nanofluids, the wetting angle decreased to 23.5° at 27 s, indicating that the increase in the surfactant concentration can reduce the

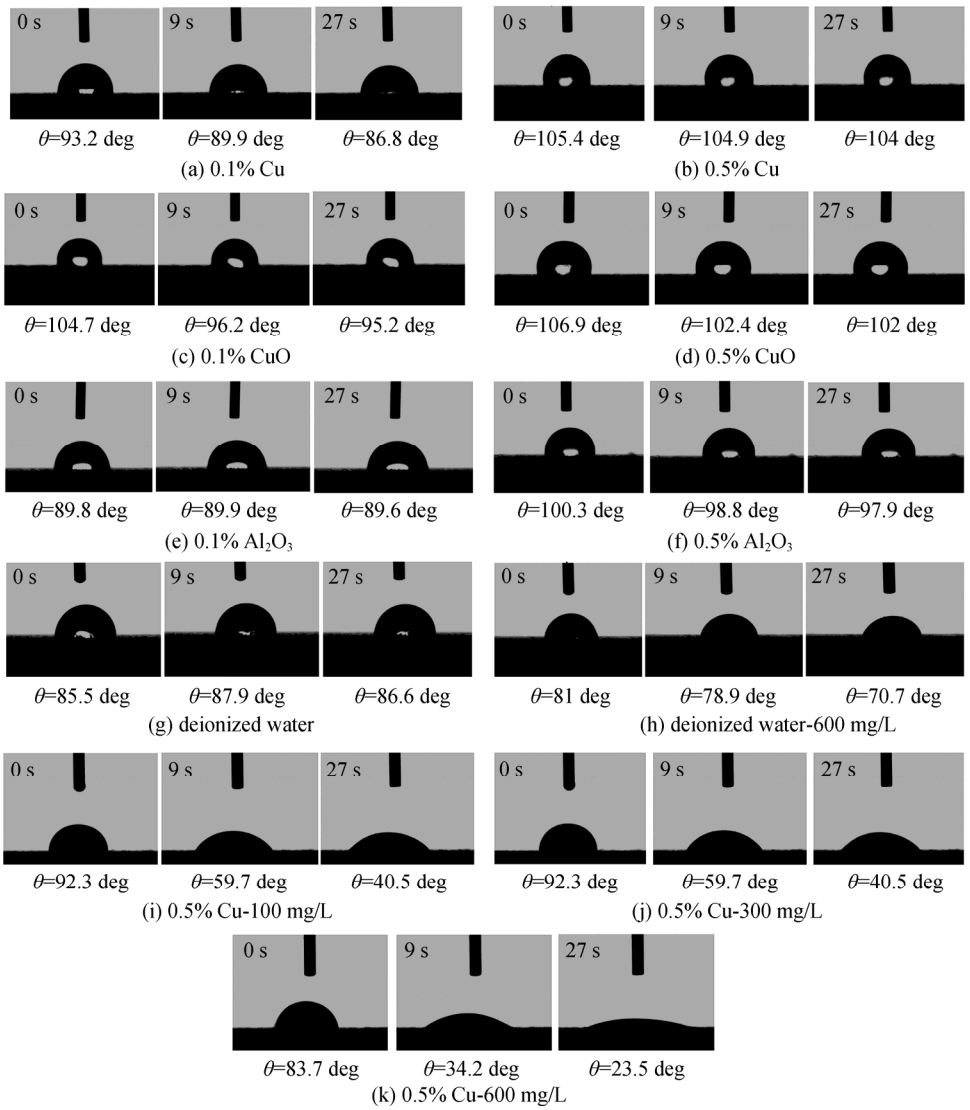

Fig. 4 Contact angles of nanoparticles with different concentrations and surfactant

surface tension of nanofluids, which in turn increases the wettability on the steel plate surface [24–26]. Moreover, the decrease in the surface tension of the coolant led to the enhancement of the heat transfer rate of the transition boiling regime as well as the critical heat flux [17, 27].

3.2. Cooling curves of different nanofluids volume fraction

When the volume fraction of Cu nanoparticles increases from 0.1% to 0.5%, the maximum heat flux q_{max} changed from 3.36 MW/m^2 to 3.48 MW/m^2 at the impinging point, which increased by 3.6%, while at r = 30 mm (r: the distance from the impinging point), q_{max} changed from 2.65 MW/m^2 to 2.83 MW/m^2, with an increase of 6.8% (Fig. 5). According to the effective-medium theory [24], the nanoparticles filled the remaining space within the base liquid molecules, which changed the internal structure characteristics of the base liquid and improved the thermal conductivity; on the other hand, the Brownian movement under the effect of nanoparticles in the base fluid led to the increased thermal conductivity of nanofluids.

At r = 30 mm, for different nanofluids with a volume fraction of 0.5%, the q_{max} values of Cu, CuO, and Al_2O_3 nanofluids at the impact point were 3.48 MW/m^2, 3.39 MW/m^2, and 3.26 MW/m^2, respectively, with corresponding time t_{max} values of 12.8 s, 13.6 s, and 14.8 s, indicating that the heat transfer efficiency follows the order of Cu nanofluids > CuO nanofluids > Al_2O_3 nanofluids. The thermal conductivities of Cu, CuO, and Al_2O_3 are 377 W/(m·K) [28], 76.5 W/(m·K) [29], and 46 W/(m·K) [30], respectively; hence, nanoparticles with high thermal conductivity are more beneficial to heat transfer.

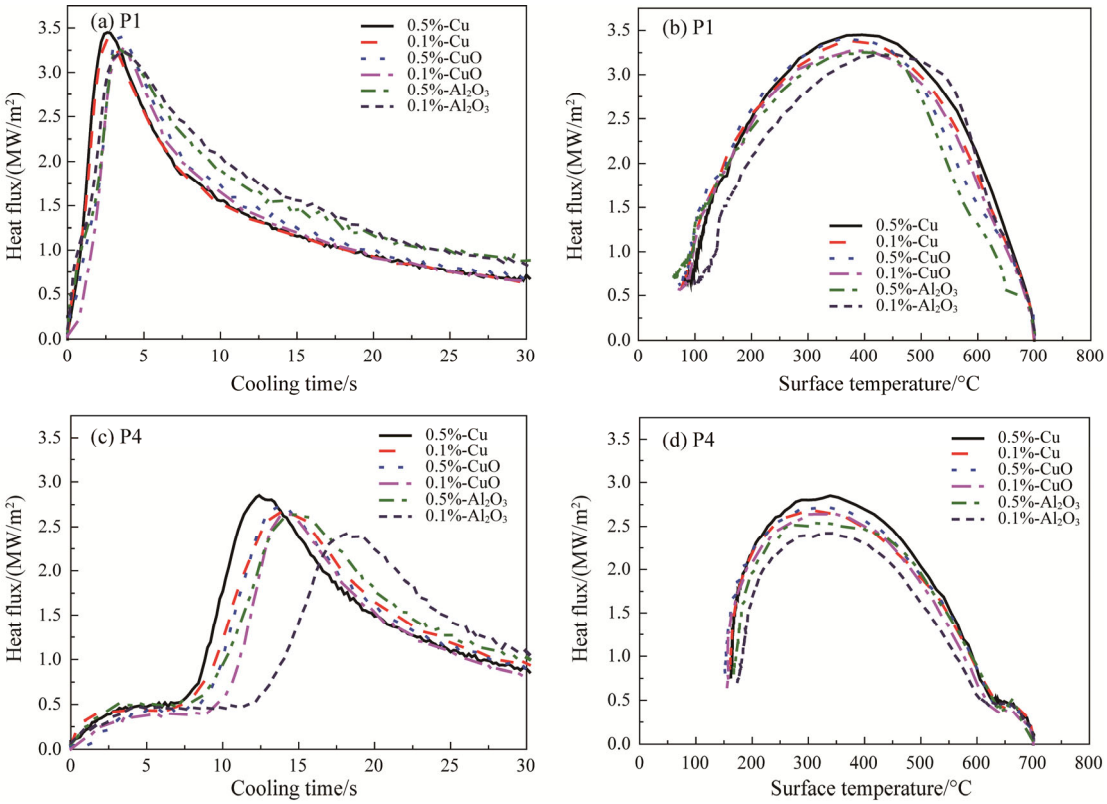

Fig. 5 Boiling curves at different positions using different nanofluids: (a) and (b) impinging point, (c) and (d) r=30 mm.

Fig. 5(b) and (d) show the boiling curves at different positions for different nanofluids. In the impingement area, the heat flux first increased and then decreased with decreasing temperature. For the same nanofluid, the maximum heat flux q_{max} and the corresponding surface temperature T_{max} increased with the volume fraction because when the droplets impacted the high temperature surface, a vapor film layer was formed on the steel plate surface, hindering the heat transfer between the cooling fluid and plate. With the progress of the heat transfer, the heat transfer mechanism changed from the film boiling heat transfer mechanism to nucleate boiling and transition boiling heat transfer stages. With the increase in the number of liquid droplets, the "two nucleation" intensified heat transfer [31], which rapidly improved heat flux until it reached q_{max}. The T_{max} values of different nanofluids ranged from 400 to 420°C at the impact point, while that of conventional spray cooling was 321°C, indicating that the removing heat ability of nanofluids is better than that of deionized water under spray cooling conditions (Fig. 5(b)).

3.3. Cooling curves influence by surfactants

Fig. 6 shows the boiling profiles of working fluids used in this experimental study. Initially, the curves increased with time owing to transition boiling and reached the maximum heat flux value when transition boiling changed to nucleate boiling, which decreased thereafter [32]. The q_{max} values for the nanofluids with Tween 20 were greater than that without Tween 20. By the addition of 600 mg/L of Tween 20 to the nanofluids, the q_{max} at the impinging central point changed from 3.48 MW/m^2 to 3.94 MW/m^2, which increased by 13.2%. Furthermore, at r = 30 mm, q_{max} increased from 2.83 MW/m^2 to 3.39 MW/m^2, which increased by 19.8%; this result is in agreement with a reported previously result [22,33], indicating that the addition of Tween 20 leads to a better cooling performance compared with that observed for the 0.5% Cu nanofluids as the effect of contact angle is dominant, and the addition of Tween 20 leads to the decrease of the contact angle and improvement of wettability [24]. Moreover, high Tween 20 concentration led to the enhancement of heat flux because the decrease in the surface tension (Fig. 4(b), (i), (j), and (k)). The contact angle for 0.5% Cu-600 mg/L was the minimum, with a low surface tension, making atomization into fine-size droplets easy [33]; hence, the fluid motion is considerably easier to form broader, thinner droplets, with higher evaporation rates on the hot surface [34], leading to increased heat transfer. In addition, the surfactant was adsorbed on the nanoparticle surface, forming an adsorption layer, which not only increased the distance between particles, thereby decreasing the Hamaker constant, but also the overlapped

the adsorbed layer, affording a new repulsion that decreases the van der Waals gravitational potential energy between the nanoparticles [35]. Thus, the surfactant hinders the agglomeration of nanoparticles and increases the number of effective particles in the volume and the frequency of collisions between particles, thereby increasing the thermal conductivity of nanofluids.

Fig. 7(a) and (b) shows the increase of heat flux with a high surfactant concentration of Tween 20 with respect to the temperature. In addition, the heat flux curves in the impact (P1) and parallel flow (P4) regions showed higher heat flux for a higher surfactant concentration. At the impinging central point, surface temperatures of the steel plate corresponding to the nanofluids with surfactant and nanofluids without surfactant were 450°C and 400°C, respectively (Fig. 7(a)).

The t_{max} (time to reach maximum heat flux) increased with the distance from the impinging point (Fig. 8(a)). With increasing surfactant concentration, the wetting delay gradually decreased. This result also revealed that, with the increase in the distance from the impinging point, the wetting delay is prolonged.

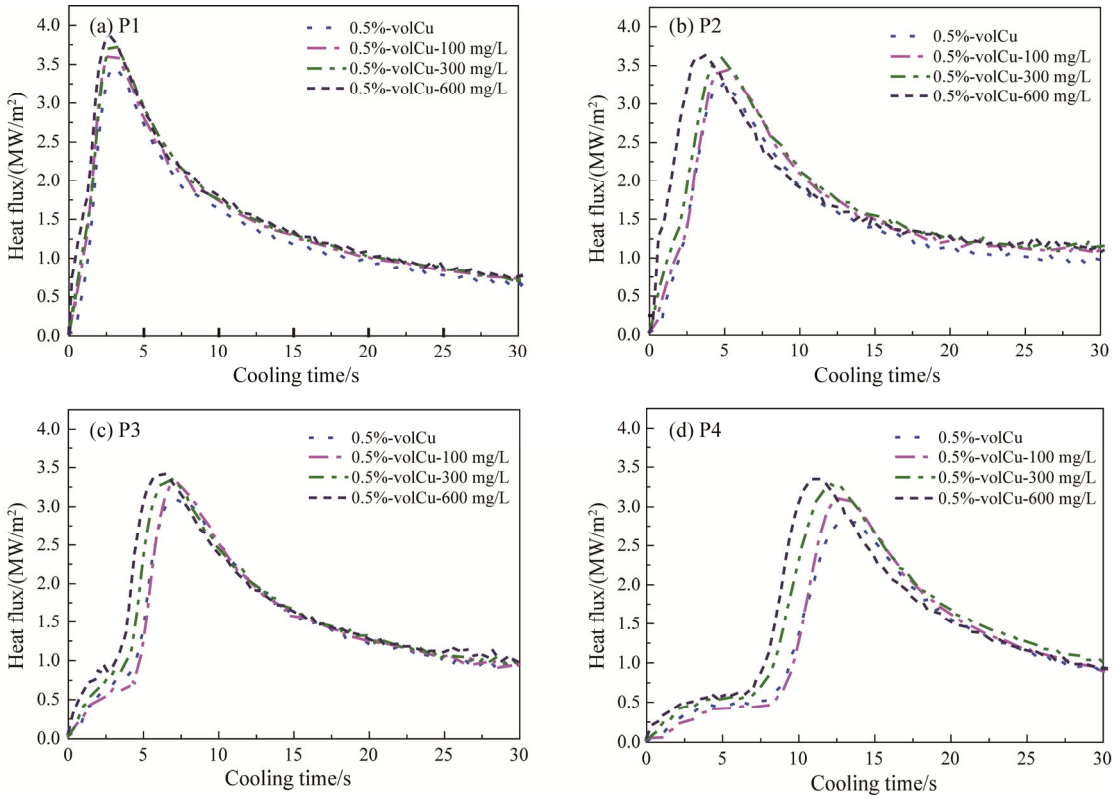

Fig. 6 Variation of surface heat flux with time at different measurement points, (a) impinging point; (b) r=10 mm; (c) r=20 mm; (d) r=30 mm

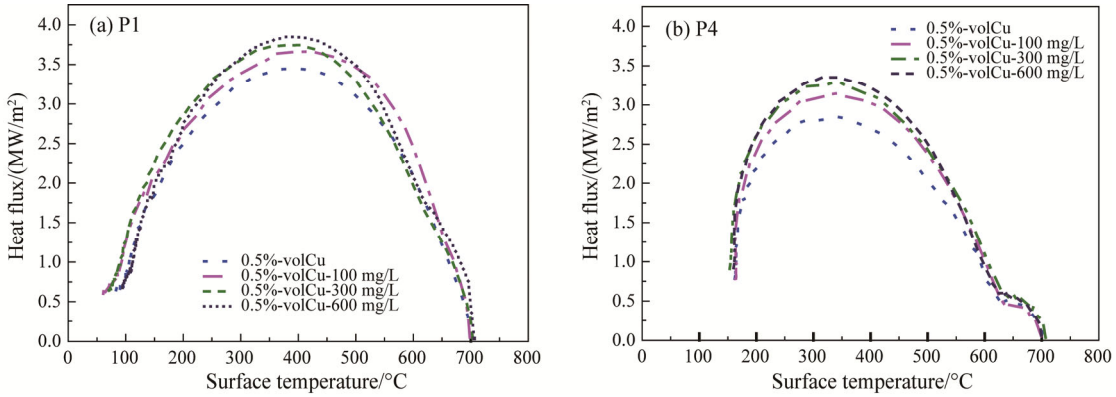

Fig. 7 Variation of surface heat flux with surface temperature at different measurement points, (a) impinging point; (b) r=30 mm

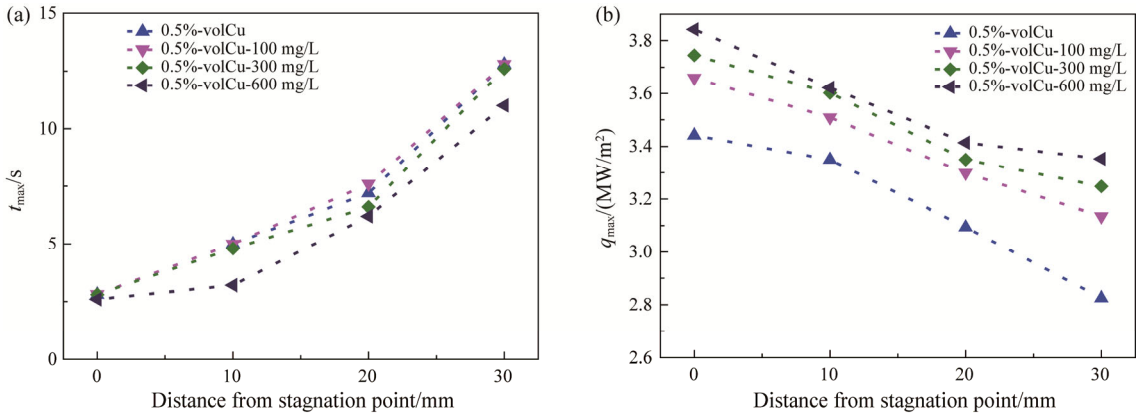

Fig. 8 t_{max} and q_{max} values at different surfactant concentrations

The hot surface quenching performance can be evaluated on the basis of the maximum heat flux, which was obtained from the surface heat flux, the maximum surface heat flux occurring at the boundary between the transition and nucleate boiling regions; in addition, q_{max} corresponded to the critical heat flux point under the pool boiling and jet impingement cooling [36]. q_{max} values at different surfactant concentrations are shown in Fig. 8(b): with increasing surfactant concentration at the impinging central point, q_{max} increased from 3.48 MW/m^2 to 3.94 MW/m^2. Surfactant not only hindered the aggregation of internal particles in nanofluids but also inhibited the surface tension of droplets, and q_{max} decreased with the increase in the distance from the impact point. The lower the surface tension, the higher the wettability of the steel surface; hence, the liquid is promoted to propagate on the steel surface and improve the heat transfer efficiency [32,37]. This result is in good agreement with that reported by Cheng et al., who also reported that heat flux increases by the addition of surfactant [38].

4. Conclusions

The following conclusions were drawn from this experimental investigation for the spray cooling of nanofluids by using different parameters:

(1) From contact angle measurements, the surfactant was found to improve the wettability of the coolant. With the increase in the volume fraction, the surfactant decreased the solid/liquid contact angle. The decreased contact angle improved heat transfer by enhancing the wettability and forming a thin deposition layer on the surface.

(2) The thermal conductivity of nanofluids increased with the volume fraction because nanoparticles optimized the thermal properties of the coolant, increased the thermal conductivity of the coolant. With the increase in the volume fraction of Cu nanoparticles from 0.1% to 0.5%, q_{max} increased from 3.36 MW/m^2 to 3.48 MW/m^2 at the impinging point. For different nanofluids with a volume fraction of 0.5%, the heat transfer efficiency followd the order of Cu nanofluids > CuO nanofluids > Al_2O_3 nanofluids.

(3) With increasing concentration of surfactant in the nanofluids, the heat flux in the cooling zone increased. The surfactant decreased the contact angle and improved the wettability; hindered nanoparticle agglomeration; increased the effective collision between the particles and steel plate; and accelerated the nucleate boiling. Hence, deionized water with 600 mg/L of the surfactant exhibited a better cooling ability than deionized water.

Acknowledgments

This research was jointly supported by National Key R & D Plan (Project No. 2017YFB0305103), National Natural Science Foundation of China (Grant No. 51404058), the fundamental research funds for the central universities (Grant No. N150704005), and the open project of the RAL at Northeastern University (Grant No. 2016006).

References

[1] Cox S.D., Hardy S.J., Parker D.J., Influence of runout table operation setup on hot strip quality, subject to initial strip condition: heat transfer issues. Ironmaking & Steelmaking, 2001, 28(5): 363–372.

[2] Chester N.L., Wells M.A., Prodanovic V., Effect of inclination angle and flow rate on the heat transfer during bottom jet cooling of a steel plate. Journal of Heat Transfer, 2012, 134(12): 122201.

[3] Xie J.L., Zhao R., Duan F., et al., Thin liquid film flow and heat transfer under spray impingement. Applied Thermal Engineering, 2012, 48: 342–348.

[4] Wongcharee K., Chuwattanakul V., Eiamsa-ard S., Heat

transfer of swirling impinging jets with TiO_2-water nanofluids. Chemical Engineering and Processing: Process Intensification, 2017, 114: 16–23.

[5] Wang Y., Liu M., Liu D., et al., Experimental study on the effects of spray inclination on water spray cooling performance in non-boiling regime. Experimental Thermal and Fluid Science, 2010, 34(7): 933–942.

[6] Aamir M., Qiang L., Xun Z., et al., Ultra fast spray cooling and critical droplet daimeter estimation from cooling rate. Journal of Power and Energy Engineering, 2014, 2(04): 259–270.

[7] Agrawal C., Lyons O.F., Kumar R., et al., Rewetting of a hot horizontal surface through mist jet impingement cooling. International Journal of Heat and Mass Transfer, 2013, 58(1–2): 188–196.

[8] Suresh S., Venkitaraj K.P., Selvakumar P., et al., Synthesis of Al_2O_3–Cu/water hybrid nanofluids using two step method and its thermo physical properties. Colloids and Surfaces A: Physicochemical and Engineering Aspects, 2011, 388(1–3): 41–48.

[9] Chakraborty S., Sarkar I., Ashok A., et al., Thermo-physical properties of Cu-Zn-Al LDH nanofluid and its application in spray cooling. Applied Thermal Engineering, 2018, 141: 339–351.

[10] Kolsi L., Hussein A., Borjini M., et al., Computational analysis of three-dimensional unsteady natural convection and entropy generation in a cubical enclosure filled with water-Al_2O_3 nanofluid. Arabian Journal for Science and Engineering, 2014, 39(11): 7483–7493.

[11] Al-Rashed A., Kalidasan K., Kolsi L., et al., Mixed convection and entropy generation in a nanofluid filled cubical open cavity with a central isothermal block. International Journal of Mechanical Sciences, 2018, 135: 362–375.

[12] Fan L.W., Li J.Q., Li D.Y., et al., The effect of concentration on transient pool boiling heat transfer of graphene-based aqueous nanofluids. International Journal of Thermal Sciences, 2015, 91: 83–95.

[13] Karimzadehkhouei M., Shojaeian M., Şendur K., et al., The effect of nanoparticle type and nanoparticle mass fraction on heat transfer enhancement in pool boiling. International Journal of Heat and Mass Transfer, 2017, 109: 157–166.

[14] Sundar L.S., Sharma K.V., Singh M.K., et al., Hybrid nanofluids preparation, thermal properties, heat transfer and friction factor–a review. Renewable and Sustainable Energy Reviews, 2017, 68: 185–198.

[15] Lee D., Irmawati N., Investigation on fluid flow and heat transfer characteristics in spray cooling systems using nanofluids. Dynamics, 2015, 9(8): 1409–1413.

[16] Jha J., Ravikumar S., Tiara A., et al., Ultrafast cooling of a hot moving steel plate by using alumina nanofluid based air atomized spray impingement. Applied Thermal Engineering, 2015, 75: 738–747.

[17] Mohapatra S.S., Ravikumar S.V., Verma A., et al., Experimental investigation of effect of a surfactant to increase cooling of hot steel plates by a water jet. Journal of Heat transfer, 2013, 135(3): 032101.

[18] Mohapatra S.S., Ravikumar S.V., Andhare S., et al. Experimental study and optimization of air atomized spray with surfactant added water to produce high cooling rate. Journal of Enhanced Heat Transfer, 2012, 19(5): 397–408.

[19] Clay M.A., Miksis M.J., Effects of surfactant on droplet spreading. Physics of Fluids, 2004, 16(8): 3070–3078.

[20] Gradeck M., Ouattara A., Maillet D., et al., Heat transfer associated to a hot surface quenched by a jet of oil-in-water emulsion. Experimental Thermal & Fluid Science, 2011, 35(5): 841–847.

[21] Drzazga M., Lemanowicz M., Dzido G., et al., Preparation of metal oxide-water nanofluids by two-step method. Inżynieria I Aparatura Chemiczna, 2012, 51(5): 213–215.

[22] Ravikumar S.V., Jha J.M., Sarkar I., et al., Mixed-surfactant additives for enhancement of air-atomized spray cooling of a hot steel plate. Experimental Thermal and Fluid Science, 2014, 55: 210–220.

[23] Zhang X., Basaran O.A., Dynamic surface tension effects in impact of a drop with a solid surface. Journal of Colloid and Interface Science, 1997, 187(1): 166–178.

[24] Jeong Y.H., Chang W.J., Chang S.H., Wettability of heated surfaces under pool boiling using surfactant solutions and nano-fluids. International Journal of Heat and Mass Transfer, 2008, 51(11–12): 3025–3031.

[25] Sarafraz M.M., Kiani T., Hormozi F., Critical heat flux and pool boiling heat transfer analysis of synthesized zirconia aqueous nano-fluids. International Communications in Heat and Mass Transfer, 2016, 70: 75–83.

[26] Khaleduzzaman S.S., Mahbubul I.M., Shahrul I.M., et al., Effect of particle concentration, temperature and surfactant on surface tension of nanofluids. International Communications in Heat and Mass Transfer, 2013, 49: 110–114.

[27] Yang Y.M., Maa J.R., Pool boiling of dilute surfactant solutions. Journal of Heat Transfer, 1983, 105(1): 190–192.

[28] Chol S.U.S., Estman J.A., Enhancing thermal conductivity of fluids with nanoparticles. Website: https://www.osti.gov/servlets/purl/196525 (accessed in 2018).

[29] Hwang Y.J., Ahn Y.C., Shin H.S., et al., Investigation on characteristics of thermal conductivity enhancement of nanofluids. Current Applied Physics, 2006, 6(6): 1068–1071.

[30] Xue Q.Z., Model for effective thermal conductivity of nanofluids. Physics Letters A, 2003, 307(5–6): 313–317.

[31] Teja A.S., Beck M.P., Yuan Y., et al., The limiting behavior of the thermal conductivity of nanoparticles and nanofluids. Journal of Applied Physics, 2010, 107(11): 114319.

[32] Ravikumar S.V., Jha J.M., Sarkar I., et al., Enhancement of heat transfer rate in air-atomized spray cooling of a hot steel plate by using an aqueous solution of non-ionic surfactant and ethanol. Applied Thermal Engineering, 2014, 64(1–2): 64–75.

[33] Bhattacharya P., Samanta A., Chakraborty S., Spray evaporative cooling to achieve ultra fast cooling in runout table. International Journal of Thermal Sciences, 2009, 48(9): 1741–1747.

[34] Crafton E., Black W., Heat transfer and evaporation rates of small liquid droplets on heated horizontal surfaces. International Journal of Heat and Mass Transfer, 2004, 47(6–7): 1187–1200.

[35] Ma X., Su F., Chen J., et al., Heat and mass transfer enhancement of the bubble absorption for a binary nanofluid. Journal of Mechanical Science and Technology, 2007, 21(11): 1813–1818.

[36] Karwa N., Experimental study of water jet impingement cooling of hot steel plates. tuprints, Darmstadt, Germany, 2012.

[37] Tseng A.A., Bellerová H., Pohanka M., et al., Effects of titania nanoparticles on heat transfer performance of spray cooling with full cone nozzle. Applied Thermal Engineering, 2014, 62(1): 20–27.

[38] Cheng L., Mewes D., Luke A., Boiling phenomena with surfactants and polymeric additives: a state-of-the-art review. International Journal of Heat and Mass Transfer, 2007, 50(13–14): 2744–2771.